Ag microparticles embedded in Si nanowire arrays: a novel catalyst for gas-phase oxidation of high alcohol to aldehyde†

Chenxi Zhang, Ping Chen, Jian Liu, Yahong Zhang, Wei Shen, Hualong Xu* and Yi Tang*

Received (in Cambridge, UK) 1st May 2008, Accepted 14th May 2008
First published as an Advance Article on the web 16th June 2008
DOI: 10.1039/b807354f

A novel catalyst of silver microparticles embedded in a silicon nanowire array support (Ag@SiNW) was prepared by an *in situ* electroless metal deposition method; it exhibited high selectivity and stability for gas-phase oxidation of high alcohol to its corresponding aldehyde.

The features of catalyst supports are usually the crucial factors to improve the performance of a catalyst by sufficiently exerting the superiority of the active species. An ideal support should possess, at least, two essential functions: (1) maintaining high dispersion of active components, and (2) facilitating the diffusion of reactants and the accessibility to active sites. Therefore, much effort has been made to create new catalyst supports that can provide an anti-sintering property and increase the accessibility to active species. Electroless metal deposition (EMD) has been intensively studied as a simple, low-cost and effective method in the microelectronics industry and fabrication of new nanostructured materials, which performs *via* an autocatalytic electrochemical redox reaction of metal ions and the matrix in the absence of any external current source.[1–6] This technique has been exploited to fabricate large-area silicon nanowire (SiNW) arrays on single-crystal Si wafers in an aqueous solution containing HF and $AgNO_3$.[7] After this fabrication process, a layer of dendritic silver wires was found on the SiNW arrays. Recently, it is noted in our laboratory that, after a simple thermal treatment, these dendritic silver wires spontaneously transformed to uniform Ag microparticles and embedded into the gaps of SiNW arrays, forming an interesting "rocks-in-forest" structure (Scheme 1). The perpendicularly growing SiNWs not only provide the barrier to the possible agglomeration of Ag dotted in them, but also provide a fully open environment with complete exposure of the Ag species. The motivation of this paper is to develop a new concept of catalyst support with an intriguing "rocks-in-forest" structure inspired by this observation.

Silver-based catalysts have long been intensively studied as oxidizing catalysts and have been applied industrially to ethylene epoxidation,[8–10] formaldehyde synthesis[11–13] and ethylene glycol to glyoxal conversion.[14,15] However, some serious problems are still preventing them from more extensive utilization. Take the commercial electrolytic silver catalyst for example, the main problems are the low catalytic activity at low temperature and the strong sintering tendency of silver species at high temperature. Most importantly, the low selectivity to selective oxidation products blocks the further development of gas-phase catalytic reactions.[16] Our group has developed a nanosilver/zeolite film/copper grid composite catalyst aiming at optimizing silver-based oxidizing catalysts.[17,18] Herein, a new idea is proposed for the preparation of silver-based catalysts by embedding silver microparticles in silicon nanowire arrays (Ag@SiNW) through an *in situ* EMD of Ag on Si powder, followed by calcination. The employment of Si powder instead of literature-reported Si wafers[7] makes the preparation process much cheaper and easily-operated. Further, the as-prepared catalyst can be used directly to catalytic reactions due to its suitable size and shape inherited from the parent Si powder. This composite catalyst was applied to the selective catalytic oxidation of 1-octanol, and an aldehyde selectivity of more than 96% was achieved in the tested temperature range while keeping sufficient catalytic activity. This composite catalyst with new structure can provide high accessible surface area, good stability and anti-sintering property for catalytic reactions.

The preparation of Ag@SiNW catalysts was based on the *in situ* EMD method, followed by an additional calcination process. Typically, 0.2 g of Si powder of 200 mesh was immersed into 25 ml of an aqueous solution containing 5.0 mol L^{-1} HF and 0.04 mol L^{-1} $AgNO_3$ in a round-ended plastic centrifuging tube. This tube was then sealed carefully and treated at 50 °C for 60 min. After the EMD process, the Si powder was rinsed with deionized water several times and dried in 70 °C for 3 h. Then the final catalyst was obtained *via* calcination at 450 °C for 2 h.

Fig. 1 shows scanning electronic microscopic (SEM) images of the morphology evolution during the Ag@SiNW preparation procedure. Fig. 1(a) illustrates the surface of the Si powder after the EMD process, followed by drying at room temperature. The Si powder is covered with large-area vertically growing SiNWs, and the reduced dendritic Ag wires lie on SiNW arrays. The main stems and branches of the Ag

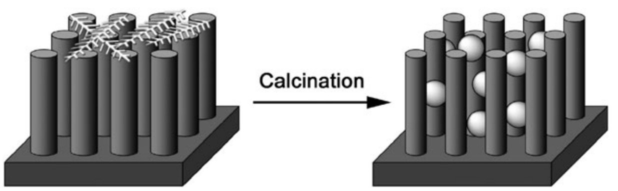

Scheme 1 Schematic depiction of Ag@SiNW formation *via* calcination. The sample after calcination shows a novel "rocks-in-forest" structure.

Department of Chemistry and Shanghai Key Laboratory of Molecular Catalysis and Innovative Materials, Fudan University, Shanghai, 200433, P. R. China. E-mail: yitang@fudan.edu.cn; Fax: +86-21-65641740; Tel: +86-21-55664125

† Electronic supplementary information (ESI) available: XRD pattern of Ag@SiNW and SEM image of Ag@SiNW at high magnification. See DOI: 10.1039/b807354f

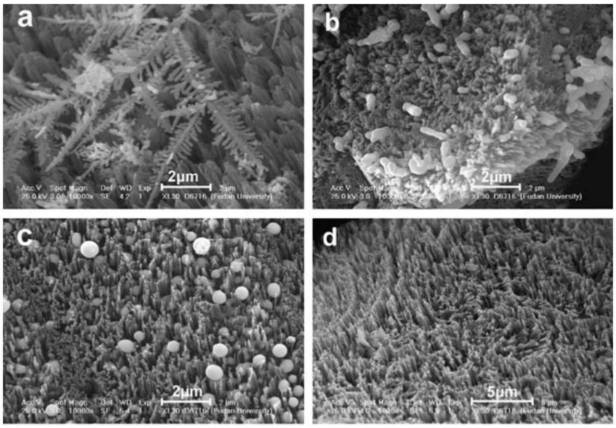

Fig. 1 SEM images of Ag@SiNW after cleansing (a), drying (b), calcination at 450 °C (c) and of SiNW arrays after removing the Ag particles (d).

dendrites are of similar sizes of *ca.* 100 nm. This situation is similar to the observation in the literature-reported EMD process for the fabrication of SiNW arrays on single-crystal Si wafers.[7] After being dried at 70 °C for 3 h (Fig. 1(b)), the symmetrical silver dendrites broke into randomly scattered short twigs due to the thermal instability of the Ag dendritic nanowires. Finally, after being calcined at 450 °C for 2 h, all of the Ag twigs further fused into uniformly dispersed microparticles, and embedded into the gaps of SiNW arrays (Fig. 1(c)). Most of the Ag microparticles were within the size range of 300–500 nm, except for a few larger ones of 600–700 nm located at the ends of the nanowire arrays. X-Ray fluorescence (XRF) analysis (after calibration) shows that the Ag loading in this composite catalyst is 36 wt%, while the X-ray diffraction (XRD) pattern of the as-prepared catalysts clearly shows two sets of diffraction peaks attributed to Si and metallic Ag, respectively (see ESI†). After ultrasonic treatment at 59 kHz for 10 min, little change was observed on the morphology of Ag microparticles and SiNW arrays, showing that Ag microparticles were firmly immobilized in SiNW arrays. After immersing the catalyst in dilute HNO_3 solution, the embedded Ag particles could be removed thoroughly, and intact SiNW arrays on Si powder surface are clearly seen in the SEM image (Fig. 1(d)). Energy dispersive X-ray spectroscopy (EDS) results show that the silicon content of the sample is 99.95 mol% after HNO_3 treatment, indicating that the nanowire arrays are composed of pure SiNWs.

During the process of electroless deposition of Ag on Si in the aqueous solution of HF and $AgNO_3$, the spontaneous autocatalytic redox reactions occur simultaneously on the Si surface exposed to the etching solution. Ag^+ ions in the vicinity of Si surface capture electrons from the valence band of Si and deposit in the form of metallic Ag nuclei (cathodic reaction), while Si underneath the Ag deposits is locally oxidized into SiO_2 (anodic reaction) and immediately dissolved by HF. This process can be expressed by the following equation:[19,20]

$$4Ag^+(aq) + Si^0(s) + 6F^-(aq) \rightarrow 4Ag(s) + SiF_6^{2-}(aq) \qquad (1)$$

The mass ratio of Ag in the final catalyst (36%) analyzed by XRF is consistent with the value calculated from eqn (1) on the basis of the weight of $AgNO_3$ and Si powder consumed in the synthesis operation.

Progressive aggregation of Ag catalysts during catalytic operation at high temperature is one of the main problems causing the deactivation of catalysts.[12,13,21] With the purpose of testing the anti-sintering property of this composite catalyst, the as-prepared Ag@SiNW and a commercial electrolytic silver catalyst were calcined at different temperatures from 300 to 800 °C for 2 h. Within the range of 300 to 600 °C, both the size of Ag microparticles and the surface morphology of the Si powder stayed the same (*e.g.*, Fig. 1(c), calcination at 450 °C). When the calcination temperature reached 700 °C (Fig. 2(a)) the size of the Ag microparticles started to grow slightly, and the SiNW arrays became less ordered, and by 800 °C (Fig. 2(c)) this tendency was more obvious. In stark contrast, the conventional electrolytic silver catalysts were seriously sintered after treatment at the same conditions (Fig. 2(b) and (d)). Furthermore, Ag@SiNW also exhibits good mechanical and thermal stability during catalytic reactions. As shown in Fig. 2(e) and (f), the morphology of the Ag@SiNW catalyst remained almost unchanged after operation for 120 h (Fig. 2(e)), while the electrolytic silver catalyst had undergone drastic morphology change (Fig. 2(f)).

Thus far, a new Ag@SiNW composite catalyst with Ag microparticles embedded in SiNW arrays has been fabricated *via in situ* EMD, followed by calcination. With the intrinsic properties and the suitable size/shape of Si powder, this composite catalyst can be applied directly to catalytic reactions. The selective oxidation of 1-octanol, a strongly exothermic reaction, was employed as a probe reaction to test the activity and selectivity of Ag@SiNW catalysts (Scheme 2).

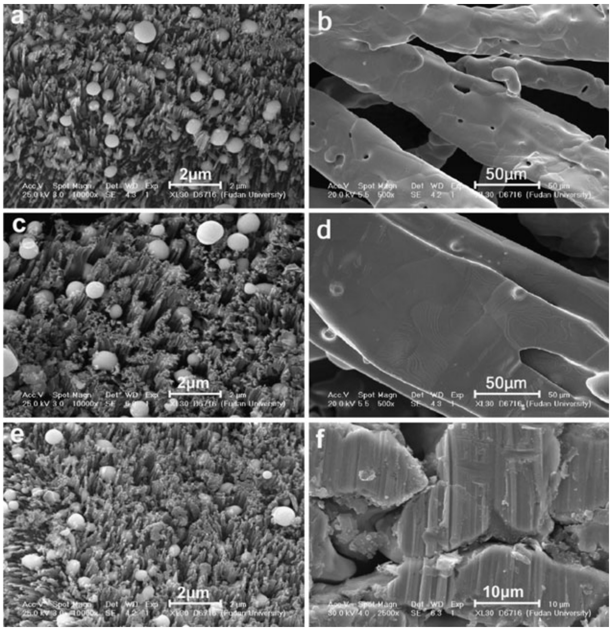

Fig. 2 SEM images of Ag@SiNW after calcination at 700 °C (a), 800 °C (c) and after reaction (e), and SEM images of electrolytic silver catalysts after calcination at 700 °C (b), 800 °C (d) and after reaction (f).

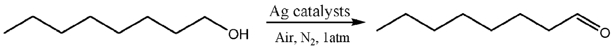

Scheme 2 Selective oxidation of 1-octanol over silver-based catalysts to its corresponding aldehyde.

Table 1 Conversion and product distribution of 1-octanol oxidation over Ag@SiNW and electrolytic silver catalysts[a]

Catalyst	T/ °C	Conversion (%)	Selectivity (mol%) 1-Octanal	Octanoic acid	C. & O.[b]
Ag@SiNW	300	65.2	96.2	3.2	0.6
	350	90.0	96.1	2.2	1.7
	400	95.5	90.8	1.5	7.7
Electrolytic Ag	300	72.2	70.3	3.3	26.4
	350	90.7	68.6	2.3	29.1
	400	97.7	47.6	1.6	50.8
Ag–Si[c]	300	41.6	84.2	1.8	14.0
	350	53.9	71.0	0.8	28.2
	400	62.4	65.3	0.5	34.2
SiNWs	400	2.1	—	—	—

[a] A continuous fixed bed reactor system was adopted; pressure = 1.0 atm; O_2/alcohol = 1.0; air flow = 70 ml min^{-1} (STP); N_2 flow = 90 ml min^{-1} (STP); amount of alcohol inlet = 6 ml h^{-1}; weight of catalyst = 0.6 g. [b] C. & O. = cracking and over oxidation products. [c] The sample was prepared by mixing electrolytic Ag and Si powder mechanically with 36 wt% Ag.

The target product of this reaction is 1-octanal, which is a food flavor with a fruit-like odor and also an important intermediate of organic synthesis for other fragrances, such as α-hexyl cinnamaldehyde, 2-heptyl-1,3-dioxolane and 4-methyl-2-heptyl-1,3-dioxolane.

Table 1 displays the relationship between the conversion/selectivity of 1-octanol oxidation and reaction temperature over Ag@SiNW and a commercial electrolytic silver catalyst. In the temperature range from 300 to 400 °C, SiNWs after removing Ag species are almost catalytically inert to this reaction as shown in Table 1. It is worth noticing that Ag@SiNW presents a much higher selectivity to the target 1-octanal product than electrolytic silver. From 350 to 400 °C, over 90% of 1-octanol reacted on Ag@SiNW, and the highest selectivity product is over 96%. For the electrolytic silver, however, a considerable amount of cracking and over-oxidation by-products (*e.g.*, CO_2) were generated and even become dominant at 400 °C. The slightly lower activity of Ag@SiNW at 300 °C was caused by the lower silver content compared with that of the electrolytic silver. For comparison, a sample of electrolytic silver mechanically mixed with Si powder (Ag–Si) with the same Ag content as Ag@SiNW was also tested at the same LHSV and temperature. As shown in Table 1, the activity of Ag@SiNW was much higher than that of Ag–Si due to its open micro-environment and stable Ag microspheres in the SiNW array support. These results indicate the efficiency of Ag@SiNW in the selective oxidation of high alcohols to their corresponding aldehydes.

In conclusion, we have reported on a novel Ag@SiNW catalyst prepared by an *in situ* EMD method, followed by calcination. The SiNW arrays on the final catalyst can well stabilize the *in situ* formed silver microparticles. This method is promising for future research and utilization as a new approach for catalyst preparation because of its effectiveness, facility, low cost and reproducibility for mass production. This catalyst shows high thermal stability at high temperature owing to its special "rocks-in-forest" structure, and exhibits excellent activity/selectivity in the gas-phase selective oxidation of 1-octanol. These results highlight the great potential of Ag@SiNW catalyst in the selective oxidation of high alcohols. Furthermore, based on the idea proposed here, a series of novel catalysts could be developed by embedding the active species into open-structured nanowire arrays as needed. Research on further designing efficient catalytic systems based on the utilization of SiNW arrays as the support is being carried out in our laboratory.

This work is supported by the NSFC (20673026, 20721063), STCMS (06DJ14006, 075211013), and the Major State Basic Research Development Program (2003CB615807).

Notes and references

1. Y. Okinaka and T. Osaka, *Electroless Deposition Processes: Fundamentals and Applications*, VCH, Weinheim, 1990.
2. P. Gorostiza, R. Diaz, F. Sanz and J. R. Morante, *J. Electrochem. Soc.*, 1997, **144**, 4119.
3. P. Gorostiza, R. Diaz, M. A. Kulandainathan, F. Sanz and J. R. Morante, *J. Electroanal. Chem.*, 1999, **469**, 48.
4. P. Gorostiza, M. A. Kulandainathan, R. Diaz, F. Sanz, P. Allongue and J. R. Morante, *J. Electrochem. Soc.*, 2000, **147**, 1026.
5. L. T. Qu and L. M. Dai, *J. Am. Chem. Soc.*, 2005, **127**, 10806.
6. H. Kind, A. M. Bittner, O. Cavalleri, K. Kern and T. Greber, *J. Phys. Chem. B*, 1998, **102**, 7582.
7. K. Q. Peng, Y. J. Yan, S. P. Gao and J. Zhu, *Adv. Mater.*, 2002, **14**, 1164.
8. M. de Carvalho, F. B. Passos and M. Schmal, *J. Catal.*, 2007, **248**, 124.
9. M. L. Bocquet, A. Michaelides, D. Loffreda, P. Sautet, A. Alavi and D. A. King, *J. Am. Chem. Soc.*, 2003, **125**, 5620.
10. M. L. Bocquet and D. Loffreda, *J. Am. Chem. Soc.*, 2005, **127**, 17207.
11. A. Nagy, G. Mestl, T. Ruhle, G. Weinberg and R. Schlogl, *J. Catal.*, 1998, **179**, 548.
12. G. I. N. Waterhouse, G. A. Bowmaker and J. B. Metson, *Appl. Catal., A*, 2004, **266**, 257.
13. M. Qian, M. A. Liauw and G. Emig, *Appl. Catal., A*, 2003, **238**, 211.
14. A. J. Capote and R. J. Madix, *J. Am. Chem. Soc.*, 1989, **111**, 3570.
15. P. Gallezot, S. Tretjak, Y. Christidis, G. Mattioda and A. Schouteeten, *J. Catal.*, 1993, **142**, 729.
16. K. Weissermel and H. J. Arpe, *Industrial Organic Chemistry*, VCH, New York, 1997.
17. J. Shen, W. Shan, Y. H. Zhang, J. M. Du, H. L. Xu, K. N. Fan, W. Shen and Y. Tang, *Chem. Commun.*, 2004, 2880.
18. J. Shen, W. Shan, Y. H. Zhang, J. M. Du, H. L. Xu, K. N. Fan, W. Shen and Y. Tang, *J. Catal.*, 2006, **237**, 94.
19. T. Qiu, X. L. Wu, G. J. Wan, Y. F. Mei, G. G. Siu and P. K. Chu, *J. Cryst. Growth*, 2005, **284**, 470.
20. K. Q. Peng, J. J. Hu, Y. J. Yan, Y. Wu, H. Fang, Y. Xu, S. T. Lee and J. Zhu, *Adv. Funct. Mater.*, 2006, **16**, 387.
21. G. Reuss, W. Disterldorf, O. Grundler and A. Hilt, Formaldehyde, in *Ullmann's Encyclopedia of Industrial Chemistry*, VCH, Weinheim, 6th edn, 2001, vol. A11.